In Situ Aircraft Measurements of the Vertical Distribution of Liquid and Ice Water Content in Midlatitude Mixed-Phase Clouds

Yoo-Jeong Noh and Curtis J. Seaman

Department of Defense Center for Geosciences/Atmospheric Research, Cooperative Institute for Research in the Atmosphere, Colorado State University, Fort Collins, Colorado

Thomas H. Vonder Haar

Department of Defense Center for Geosciences/Atmospheric Research, Cooperative Institute for Research in the Atmosphere, and Department of Atmospheric Science, Colorado State University, Fort Collins, Colorado

Guosheng Liu

Department of Earth, Ocean and Atmospheric Science, The Florida State University, Tallahassee, Florida

ABSTRACT

The vertical distribution of liquid and ice water content and their partitioning is studied using 34 cases of in situ measured microphysical properties in midlatitude mixed-phase clouds, with liquid water path ranging from near zero to ~248 g m^{-2}, total water path ranging from near zero to ~562 g m^{-2}, and cloud-top temperature ranging from $-2°$ to $-38°$C. The 34 profiles were further divided into three cloud types depending on their vertical extents and altitudes. It is found that both the vertical distribution of liquid water within a cloud and the liquid water fraction (of total condensed water) as a function of temperature or relative position in a cloud layer are cloud-type dependent. In particular, it is found that the partitioning between liquid and ice water for midlevel shallow clouds is relatively independent on the vertical position within the cloud while it clearly depends on cloud mean temperature. For synoptic snow clouds, however, liquid water fraction increases with the decrease of altitude within the cloud. While the liquid water fraction in synoptic clouds also decreases with lowering temperature, its magnitude is only about 50% near 0°C.

1. Introduction

Despite the advances in measurement instruments and scientific techniques, clouds are still one of the critical sources of uncertainty in understanding Earth's climate variability and the morphology of weather systems regarding cloud impacts on atmospheric radiation and energy balance (Houghton et al. 2001; Randall et al. 2007). Cloud liquid and ice have substantially different impacts on atmospheric radiation due to differences in particle size, shape, density, concentration, and refractive index (Sun and Shine 1994). The generalized properties of mixed-phase clouds in which liquid and ice coexist are relatively unknown and remain an active area of research. Recent studies indicate that 40%–60% of clouds in the temperature range between 0° and −30°C are mixed phase and 30%–60% are supercooled liquid water clouds (Korolev et al. 2003; Mazin 2006; Shupe et al. 2006; Zhang et al. 2010). The longevity and areal extent of these supercooled-liquid and mixed-phase clouds have a significant impact on the radiative balance (Sun and Shine 1995; DeMott et al. 2010).

In many numerical models, the liquid water fraction of total cloud condensates is prescribed according to some temperature relationships that have a limited physical basis. While the homogeneous freezing point of water in cloud (the temperature below which water will not exist as liquid) has been found to be near −40°C (with a dependence on droplet size, chemical composition, and ambient vertical velocity; Heymsfield and Miloshevich 1993; Heymsfield et al. 2005; Swanson 2009), many

Corresponding author address: Yoo-Jeong Noh, Cooperative Institute for Research in the Atmosphere, 1375 Campus Delivery, Colorado State University, Fort Collins, CO 80523-1375.
E-mail: yoo-jeong.noh@colostate.edu

numerical models limit liquid water to exist at relatively warm temperatures, for instance, specifying thresholds of $-23°C$ by Tiedtke (1993), $-15°C$ by Smith (1990) and Boucher et al. (1995), and even $-9°C$ by Gregory and Morris (1996) to discriminate between liquid and ice, as reviewed by Shupe et al. (2008). Similar temperature thresholds are also found in various remote sensing retrieval algorithms, such as the *CloudSat* water content algorithm (Noh et al. 2011). Since liquid water is actually observed in clouds at temperatures below these thresholds, many models underestimate cloud liquid in the mid- and high latitudes (Hogan et al. 2003; Hu et al. 2010). In a study of Arctic stratus clouds, Shupe et al. (2006) found, for a given liquid-to-ice ratio, a 20°C or more temperature range over which that ratio was observed, suggesting that the partitioning of phase is not simply a function of temperature. In addition, numerous in situ and remote sensing studies of stratiform mixed-phase clouds (Platt 1977; Fleishauer et al. 2002; Hogan et al. 2003; Wang et al. 2004; Zuidema et al. 2005; Shupe 2007; Ansmann et al. 2008; de Boer et al. 2008; Niu et al. 2008; Carey et al. 2008; Noh et al. 2011) have shown that supercooled liquid water often occurs in discrete layers at or near cloud top, where the lowest temperatures exist.

As discussed by Shupe et al. (2008), one of the outstanding limitations in remote sensing of mixed-phase cloud properties is a lack of knowledge of the vertical profile of cloud liquid amount. At present, there are no generally relevant methods to provide vertical profile information of liquid microphysics or estimate layer-averaged values such as liquid droplet effective radius, especially more inaccurate in optically thick cloud conditions. Detailed in situ microphysical observations from aircraft can potentially fill in this knowledge gap. Relationships between liquid water content (LWC) and temperature have been investigated using aircraft observations during several intensive field campaigns (Gultepe and Isaac 1997; Gultepe et al. 2002). A parameterization for particle number concentrations versus temperature was also studied based on those field measurements and suggested for modeling studies (Gultepe et al. 2002). Korolev et al. (2007) compiled airborne microphysical observations from 584 vertical profiles of stratiform mixed-phase clouds collected during five field experiments that took place between 1995 and 2004. They found a slight majority (55%) of the clouds had liquid layers less than 500 m thick that were usually quasi-adiabatic, while clouds thicker than 500 m had average liquid water content profiles that were nearly constant with height. The average LWC for clouds thicker than 500 m was not related to cloud depth, and averaged 0.14 g m^{-3}.

The purpose of this study is to help expand the observational knowledge base of the vertical characteristics of cloud liquid and ice in mixed-phase clouds through the analysis of vertical profiles collected in two recent field experiments during cold seasons. Cloud properties including cloud depth, temperature, LWC, and ice water content (IWC) are analyzed from 34 vertical profiles collected during the 9th and 10th Cloud Layer Experiment (CLEX) field experiments (Carey et al. 2008; Noh et al. 2011). Since a flight ascent or descent vertically through an entire cloud layer did not occur frequently during those field experiments, the sample size of this study limits the applicability of this dataset into areas such as global cloud statistics or global model cloud parameterizations. The results presented herein are intended to serve as a supplement to Korolev et al. (2007) and other similar studies on the vertical distributions of liquid and ice in mixed-phase clouds. It is the goal of this work to improve our understanding of the variety of clouds occurring in the real atmosphere and obtain observational examples, in particular, for satellite retrievals or validation of regional-scale model simulations.

2. Data

Airborne microphysical probe measurements during two intensive field experiments (during cold seasons) are analyzed in order to better understand the microphysical structures of supercooled liquid water droplets in mixed-phase clouds. These measurements were collected during CLEX-9 (Carey et al. 2008) and CLEX-10 (Noh et al. 2011). The CLEX program is part of an ongoing effort into the study of nonprecipitating, midlevel, mixed-phase clouds funded by the U.S. Department of Defense's Center for Geosciences/Atmospheric Research. The observations included in these datasets are primarily of altocumulus (Ac) and altostratus clouds (As), although a few profiles were obtained in deep, snow-producing nimbostratus (Ns).

CLEX-9, which focused on nonfrontal, nonorographic, midlevel, mixed-phase clouds, took place over the western Great Plains of the United States (eastern Wyoming and western Nebraska) from 8 October through 4 November 2001. During this experiment, the University of Wyoming King Air research aircraft (Carey et al. 2008; Niu et al. 2008) flew 10 flight missions during eight different days. Microphysical instrumentation on the King Air included a Particle Measuring Systems (PMS) Forward Scattering Spectrometer Probe (FSSP; Knollenberg 1981), a Rosemount icing detector (Cober et al. 2001), a Gerber PVM-100A (Gerber et al. 1994), and Droplet Measurement Technology (DMT) model LWC-100. These

probes provided simultaneous observations of liquid water content. In this work we use the LWC measured by the Gerber PVM-100A, which was processed following the method of Fleishauer et al. (2002). Extensive analysis performed by Carey et al. (2008) and Niu et al. (2008) showed maximum differences between the various LWC measurements to be less than 30%. Measurements of IWC were obtained from the PMS two-dimensional cloud and precipitation (2D-C and 2D-P, respectively) probes (Knollenberg 1981) following the procedure of Fleishauer et al. (2002), which utilizes the ice mass–dimensional relationship of Mitchell et al. (1990). The IWC measurements presented here have an estimated error of less than 50% (Carey et al. 2008).

CLEX-10 was performed in collaboration with the Canadian *CloudSat/Cloud–Aerosol Lidar and Infrared Pathfinder Satellite Observations* (*CALIPSO*) Validation Experiment (C3VP; Barker et al. 2008; Noh et al. 2011), which took place in southern Ontario and Quebec, Canada, between 31 October 2006 and 1 March 2007. In this joint experiment, the Canadian National Research Council (NRC) Convair-580 research aircraft flew 28 flight missions on 26 days targeting mid- and low-level, mixed-phase clouds. The Convair-580 research aircraft was equipped with a number of microphysical instruments, including redundant FSSP-100 probes, a King hot-wire probe (King et al. 1978), a Nevzorov total water content (TWC) probe (Korolev et al. 1998), a Rosemount icing detector as well as 2D-C and 2D-P probes. In this work, we show LWC measurements from the King probe, which is estimated to have errors less than 10% (Barker et al. 2008). Measurements of IWC were derived from the Nevzorov TWC probe, which has an estimated accuracy of 10%–20% (Korolev et al. 1998; Korolev and Strapp 2002). It should be noted that the accuracy of the Nevzorov and King probes in mixed-phase clouds is an area of active research. Ice particle shattering on the surface of the probes may lead to an underestimation of IWC by the TWC sensor on the Nevzorov probe and an overestimation of LWC by the King probe (Korolev et al. 2008), although these effects have not been well quantified. A calibration method of Korolev and Strapp (2002) tested in icing wind tunnels for air speeds typical for the Convair-580 has been used to derive LWC and IWC considering the residual effect of ice on the liquid sensors. In this study, 34 vertical profiles were sampled in various mixed-phase clouds that contain both liquid and ice hydrometeors, including 4 profiles from CLEX-9 and 30 profiles from CLEX-10/C3VP. Profiles were selected from spiral and en route ascents or descents through each entire cloud layer, by examining Ka-band airborne radar images along with the microphysical data. Profiles were included if both the radar images and microphysical

probe data indicated the aircraft started and ended its vertical ascent or descent above or below the cloud layer. Since we used data from two different field experiments that took place with different aircrafts and instruments, only four midlevel cloud profiles for CLEX-9 that have approximately similar patterns and microphysical quantities (water contents and temperatures) with midlevel cloud profiles from CLEX-10/C3VP were chosen by examining each profile. It is noted that "mixed phase" clouds in this study represent clouds containing both ice and liquid regions when spatially averaging. Detailed microphysics of genuine mixed-phase clouds where ice particles and liquid droplets are uniformly mixed down to microscale has not been investigated. Also, melting particles are not considered. It should be also noted that the definition of a cloud in this study is phenomenologically based rather than microphysical process based. Cloud base and cloud top were determined by the lowest and highest altitudes where the total water content exceeded 0.005 g m^{-3}. Values of TWC less than 0.005 g m^{-3} were assumed to be clear air (Korolev et al. 2007). Multilayer clouds were separated into distinct profiles. Also, the leg period for one single profile was not over 30 min (less than 15 min for midlevel clouds) to reduce the effect of spatial inhomogeneity of the clouds, and no more than four vertical profiles were included from a single flight so as not to give undue weight to a single cloud when compiling statistics. As aircraft are unable to obtain truly vertical profiles, these soundings should be considered to be quasi-vertical, which may lead to differences due to spatial variations, as Korolev et al. (2007) indicated.

The 34 vertical profiles have been classified into three cloud categories based on their geometric thickness and temperature. Each flight report was also used to determine the weather conditions. Midlevel clouds are clouds with cloud top and cloud base between 2 and 7 km above ground (Houze 1993), which we classify further as shallow ("mid–shallow") or deep ("mid–deep"), using the thresholds for the geometric thickness of 1.5 km and the temperature difference in a cloud layer of 10°C. Thus, mid–shallow clouds would have less variety in the vertical in terms of thickness and temperature. Clouds with thickness greater than 3.5 km and with bases lower than 2 km are indicated as "synoptic snow/convective," which were associated with synoptic snowfall or deep convection (typically nimbostratus). The distinction between midlevel and deep convective clouds was made directly by flight reports and since the patterns were very different among the midlevel clouds when examining each profile, we determined that the deep and shallow clouds should be separated. Three vertical profiles were also obtained in clouds with top and base below 3 km, which were identified as lake-effect snow events by the

TABLE 1. Statistics of vertical cloud profiles for three cloud classifications derived from data during CLEX-9 and CLEX-10. Of the 34 profiles collected, 23 were mid–shallow, 6 were mid–deep, and 5 were synoptic snow.

	Cloud-base height (km)	Cloud-top height (km)	Cloud depth (km)	LWP (g m^{-2})	TWP (g m^{-2})	Cloud-base temperature (°C)	Cloud-top temperature (°C)
Mixed–shallow							
Min	1.93	2.64	0.15	0.02	4.75	−33.2	−37.9
Max	6.10	6.84	1.37	111.15	111.82	3.8	−2.1
Avg	4.00	4.66	0.66	39.16	46.81	−15.3	−19.5
Mixed–deep							
Min	2.18	4.28	1.63	0.33	20.95	−19.3	−34.2
Max	5.59	7.41	2.50	110.70	148.93	−8.6	−18.0
Avg	3.70	5.68	1.98	50.96	74.13	−14.8	−26.0
Synoptic snow							
Min	1.05	4.82	3.76	15.13	70.01	−15.8	−37.0
Max	1.66	7.07	6.00	248.00	562.03	1.9	−23.1
Avg	1.23	6.49	5.26	77.71	241.92	−8.8	−31.1

flight report, but they were not included in this study since the statistics of these profiles relative to a large sample of lake-effect snow clouds remains unclear. In the next section, we analyze the vertical distributions of cloud properties such as LWC, IWC, and temperature for each of the three cloud categories. The liquid water path (LWP) and total water path (TWP) (the integral of the LWC and TWC with height, respectively) have been calculated following the method of Korolev et al. (2007).

3. Measured profiles

The maximum, minimum, and mean values of cloud geometric and microphysical properties for the profiles in each cloud classification are shown in Table 1 and Fig. 1. Each profile contained supercooled liquid water and had cloud-top temperatures below 0°C. All but 2 of the 34 profiles had a cloud-base temperature below 0°C. The synoptic snow profiles had the lowest total liquid water fraction (ratio of liquid water path to total water path, LWP/TWP). The average total liquid water fraction of synoptic snow cases was 36%. Shallow midlevel, mixed-phase clouds had an average total liquid water fraction of 73%, while this fraction was smaller in the deeper midlevel clouds (53%), indicating the deeper clouds typically contained more ice than the shallow clouds. It should be noted that there exists an order of magnitude (or more) variability in the cloud water paths within the different classifications. While 29 of the 34 profiles are from midlevel, mixed-phase clouds (shallow and deep combined), there was no significant linear relation between cloud depth and LWP or TWP for the observed profiles in this study. The R-squared correlation coefficients were 0.02 and 0.15, respectively, and not proportional to depth squared either.

Sample profiles of LWC, IWC, and temperature are represented in Fig. 2 for three cloud categories. Figure 3

shows the distributions of LWC and IWC versus height or temperature using all the profiles for the mid–shallow and mid–deep midlevel clouds and the synoptic snow/convective clouds. LWC and IWC profiles in these
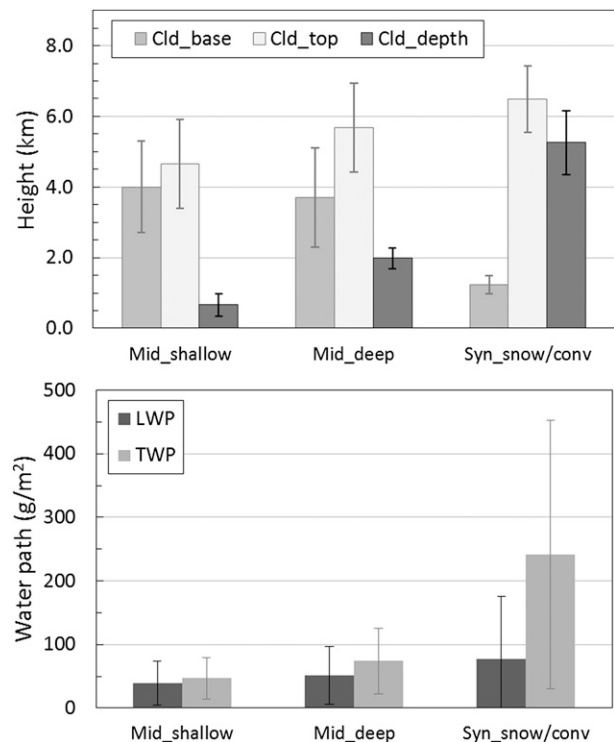

FIG. 1. Averages of (top) cloud base, top, and depth with (bottom) LWP and TWP for 34 profiles examined using radar and flight tracks that are separated into three groups: shallow midlevel, mixed phase (less than 1.5 km thick and less than 10°C temperature difference in a cloud layer); deep midlevel, mixed phase (>1.5 km thick); and synoptic snow/deep convective mixed-phase clouds (e.g., nimbostratus). Note that the error bars represent each standard deviation among the means.
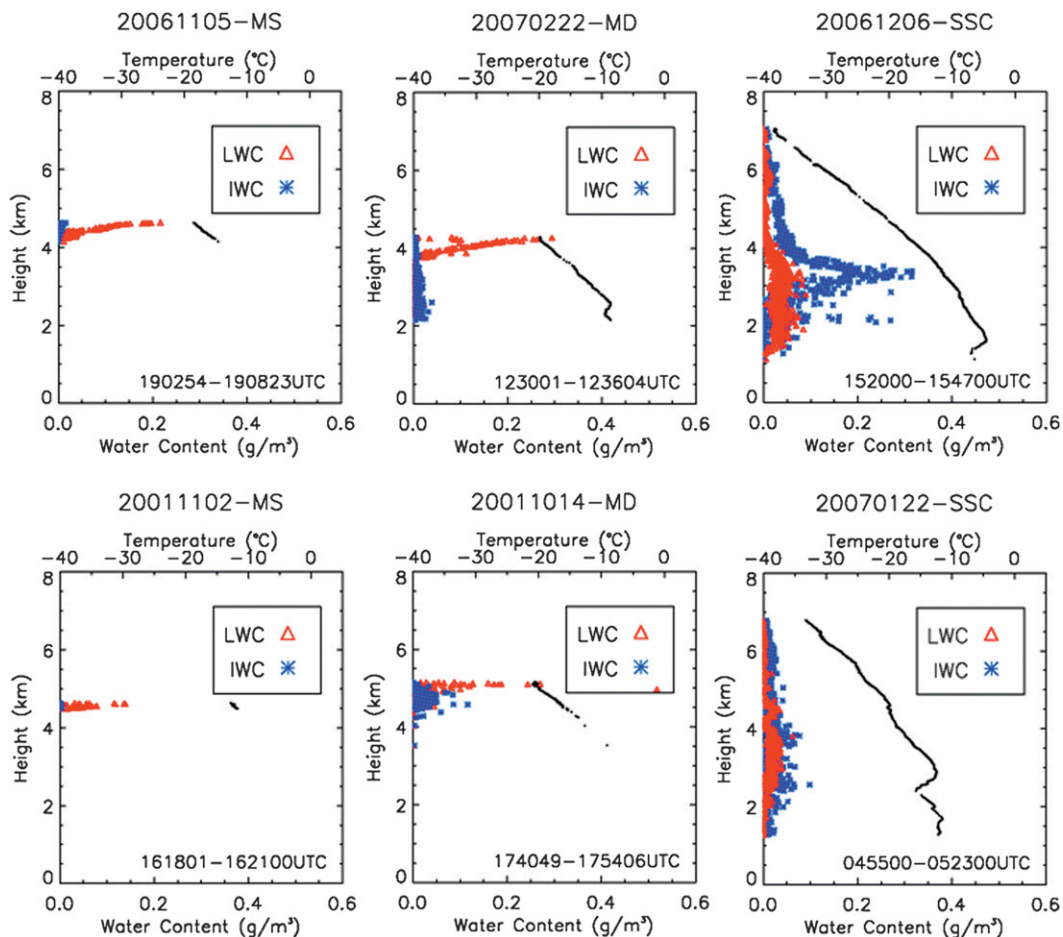
FIG. 2. Sample profiles of LWC (red triangles) and IWC (blue asterisks) with temperatures (black dots) for three cloud categories: (left) mid–shallow (top) 5 Nov 2006 and (bottom) 2 Nov 2001; (middle) mid–deep (top) 22 Feb 2007 and (bottom) 14 Oct 2001; and (right) synoptic snow/convective (top) 6 Dec 2006 and (bottom) 22 Jan 2007.

figures particularly for midlevel clouds show similar patterns and amounts with sample profiles shown in Fleishauer et al. (2002) and Korolev et al. (2007), although those measurements are from different in situ campaigns that took place over different regions and time periods. Please note that convective clouds have not been considered in those studies. Significant amounts of liquid water were observed at heights as high as 7 km and temperatures as low as $-35°$C. For the synoptic snow/convective clouds, larger IWC values were generally observed throughout the cloud profiles and much smaller amounts of IWC (<0.8 g m^{-2}) were found for the mid–deep cloud profiles. However, the dependency of LWC on height or temperature is less obvious in these plots.

4. Results and discussions

One way to show the common features in vertical distributions of water content is to composite cases in each cloud category, which is done in this study by transforming cloud layer to a dimensionless vertical coordinate from 0 (cloud base) to 1 (cloud top), and averaging related variables in the new coordinate (called normalized height in this paper) as shown in Fig. 4. In Fig. 4a, we show the vertical profiles of LWC normalized by LWP/depth (this normalization factor makes sure that the vertical integration of the normalized LWC is 1 for each case). This normalized LWC is the probability distribution (in the vertical) of LWC if the LWP value is given (e.g., measured by microwave radiometers). For synoptic snow profiles, LWC generally increases with the decrease of height, resulting in the highest LWC values appearing in the lower portion of the cloud layer. For shallow midlevel clouds, the opposite is true; that is, LWC has higher values near cloud top, similar to the result published by Carey et al. (2008). The existence of significant amounts of supercooled liquid water has been also found in Arctic boundary layer clouds studied in
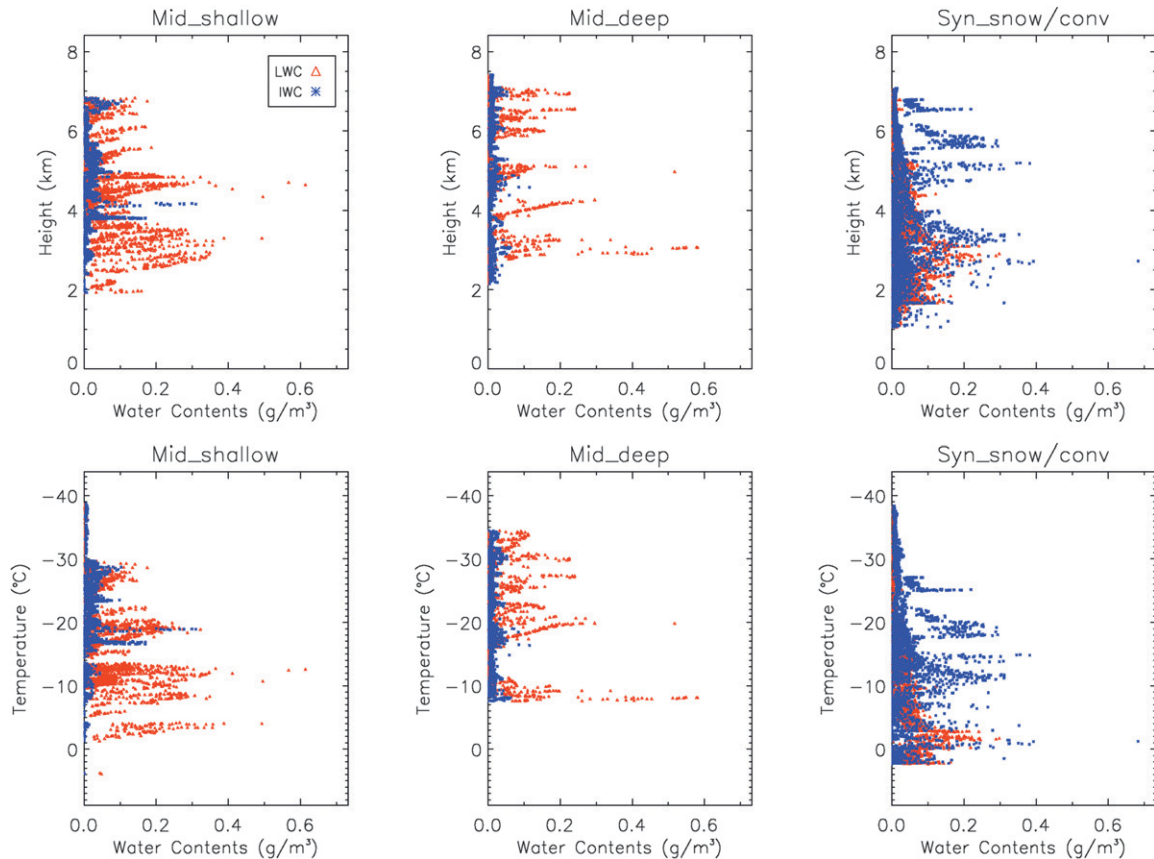
FIG. 3. Scatterplots of observed LWC and IWC values vs (top) height and (bottom) temperature, separated by (left to right) the three cloud categories.

Shupe et al. (2006). For deep midlevel clouds, the LWC shows a bimodal distribution: one near cloud top and one near cloud base. In Fig. 4b, we show the vertical distribution of the ratio of LWC/TWC (i.e., the fraction of the total condensed water that is liquid). Similarly, the height has been normalized relative to cloud top and cloud base such that the cloud-base height is 0 and the cloud-top height is 1. Again, it shows that the vertical variation of the liquid fraction is cloud type dependent. For the synoptic snow clouds, there is a clear trend toward increasing liquid fraction with decreasing height within a cloud. For shallow midlevel clouds, however, the liquid fraction seems to be quasi-constant throughout the cloud layer; although the magnitude of the fraction can be very different among different cases (we will show later that this liquid fraction difference is a consequence of cloud temperature difference among these shallow cloud cases). There seems to be a trend toward increasing liquid water fraction with height for deep midlevel cloud, while a double-layered feature can also be seen in this type of clouds.

As discussed in the introduction, the dependence of the ratio of LWC/TWC on temperature has been

parameterized in many numerical weather prediction and climate models. This dependence is studied here using the in situ observed data and is shown in Fig. 5, separated by cloud category. Except for midlevel deep clouds, the liquid water fraction shows clear temperature dependence (i.e., lowering fraction with decreasing temperature). However, the rate by which the fraction lowers varies with cloud type. For shallow midlevel clouds, the majority of cloud water exists as liquid at temperatures warmer than −10°C, while its fraction is less than 50% for synoptic snow clouds at the same temperature. More interestingly, the temperature dependence of liquid fraction is clearly a result of different factors between midlevel shallow and synoptic snow clouds. As shown in Fig. 4b, the average liquid water fraction does not vary significantly vertically. Additionally, the temperature range within a cloud layer is small because these clouds are shallow (see Table 1). Therefore, the temperature dependence of the liquid water fraction shown in Fig. 5 is largely a consequence of the superposition of the 23 different cases that happened to have a broad temperature range. In other words, the
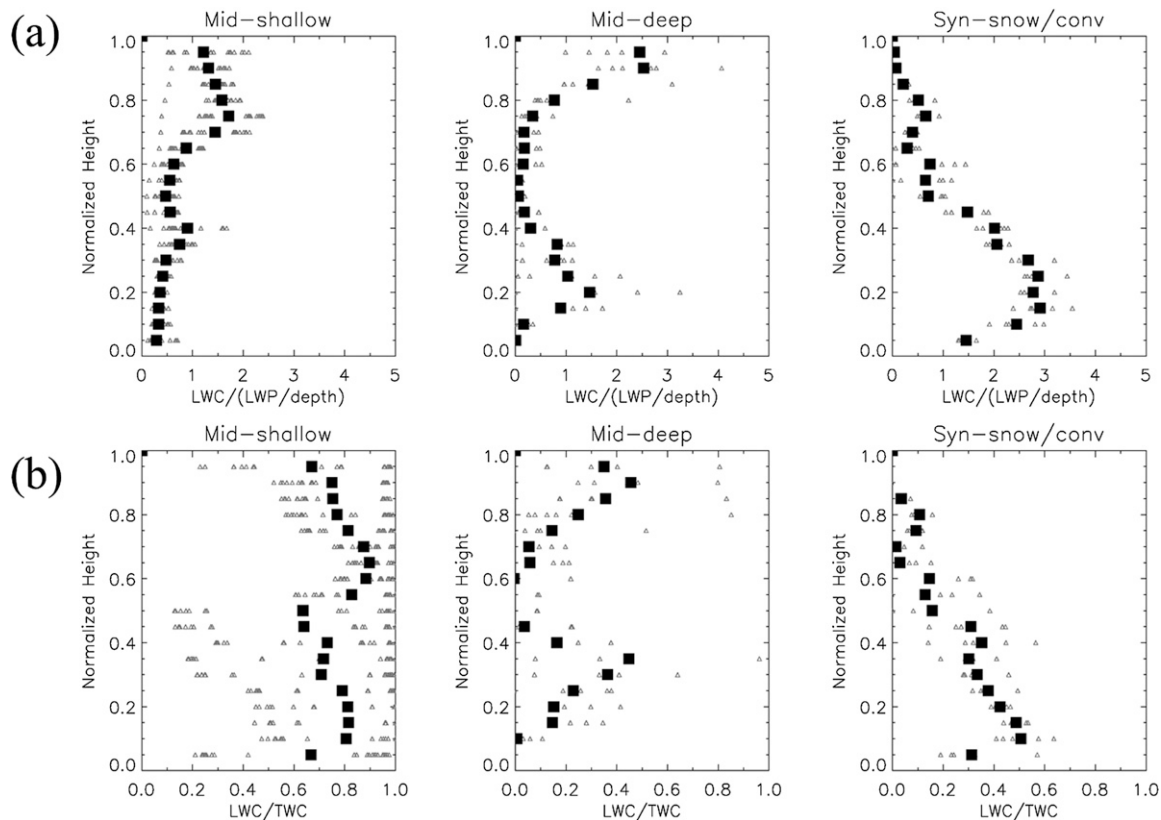
FIG. 4. Vertical distributions of (a) LWC normalized by LWP/depth and (b) the ratio of LWC/TWC for (left to right) the three cloud categories. The large black squares are the mean profiles in corresponding cloud categories. Small triangles are for individual cases. The vertical axis is normalized, so that cloud base is 0 and cloud top is 1 under the "normalized height" in every case. Each profile was three-point moving averaged per 0.05 normalized height, and 0 values were not plotted.

liquid water fraction of a midlevel shallow cloud can be largely determined by its mean temperature, while within the cloud layer there is no clear trend in liquid water fraction with respect to vertical position. For synoptic snow clouds, however, the temperature dependence of the liquid water fraction is manifested within the same cloud layer. Since temperature is warmer at lower altitude in the clouds, the liquid water fraction is also greater
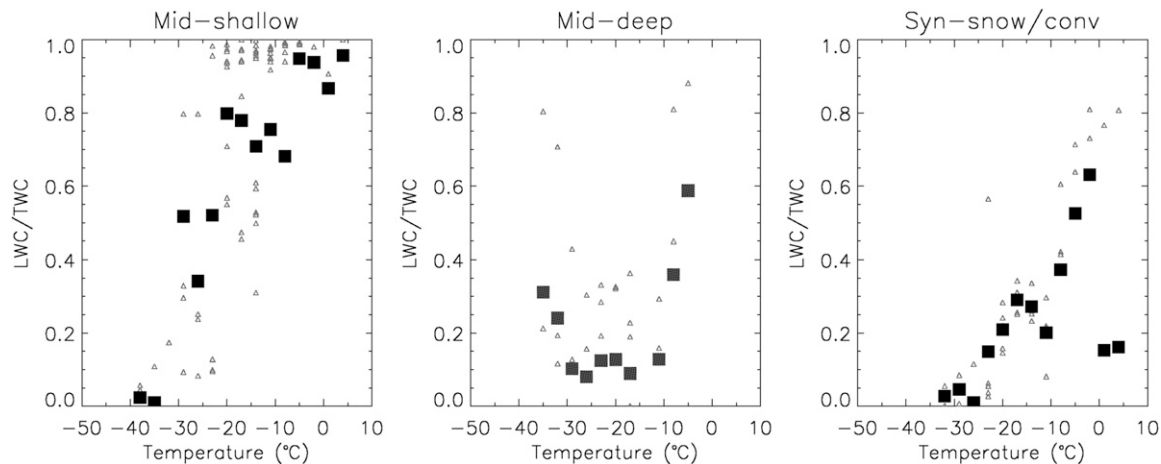

FIG. 5. The dependence of LWC/TWC ratio on temperature for (left to right) the three cloud categories. Small triangles are for individual cases, and the large black squares are the mean values under corresponding temperatures.
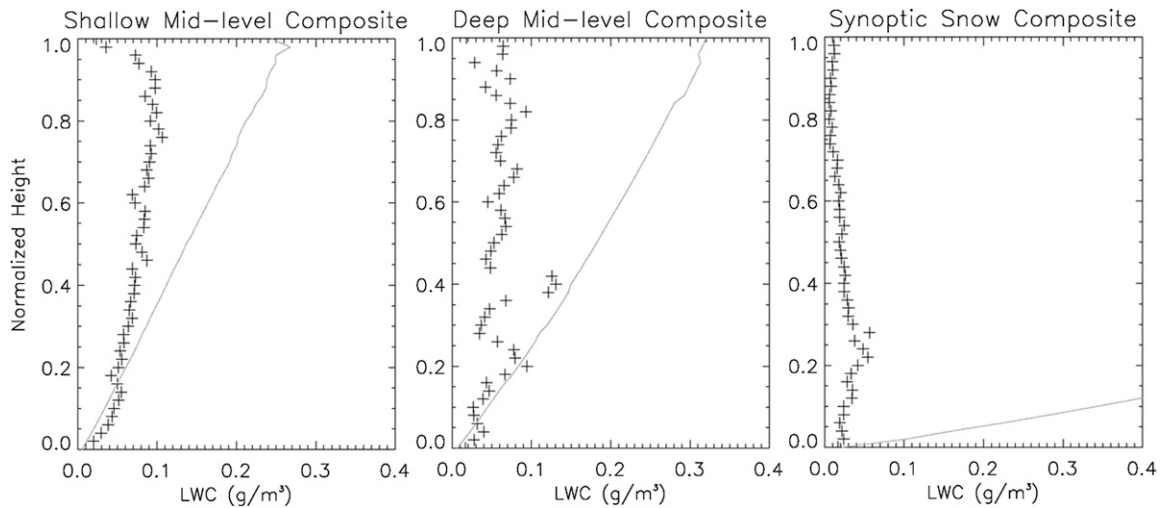
FIG. 6. Comparison of measured LWC (cross symbols) and adiabatic values (solid lines) for (left to right) the three cloud categories.

as height decreases. The lower liquid water fraction in synoptic snow clouds than that for midlevel shallow clouds at the same temperature may be due to ice particles generated at upper levels falling through the deep cloud layer below. We could not find a plausible explanation for the nondependence of the liquid water fraction on temperature for the midlevel deep clouds. Profiles in Fig. 4 indicate a discontinuity of LWC near the middle of the midlevel deep clouds, suggesting a decoupling between the top and bottom portions of the clouds, which may have complicated the LWC/TWC ratio versus temperature relation.

The profile of LWC is expected to be a function of both height and temperature, assuming the clouds are formed by adiabatic ascent, although this is complicated by the presence of ice. To determine the "adiabaticity" of these clouds, the observed LWC profiles were composited together and compared with a composite theoretical adiabatic liquid water content. Figure 6 shows the composite profiles of the observed and adiabatic LWCs for each cloud type. These composite profiles were derived by dividing each individual cloud profile into 50 layers, each layer representing 2% of the total cloud thickness. The LWC values in each layer were averaged together to form the composite profiles. The adiabatic LWC was calculated as in Rogers and Yau (1989). The LWC profiles in the shallow midlevel clouds are closer to the adiabatic profiles than the deep midlevel and synoptic snow profiles. This is consistent with the observation that the shallow midlevel clouds had the highest liquid water fractions. The lower liquid water fractions (meaning higher ice water fractions) in the mid–deep and synoptic snow profiles indicate that more water vapor is deposited on ice particles and,

therefore, less water vapor is available for the liquid droplets.

Although any generalization or significant statistics cannot be made due to the lack of samples, based on the above results, it is plausible to conclude the following. For midlevel shallow clouds, the vertical distribution of the condensed water content is largely determined by condensation–deposition of excess water vapor produced by upward air motion. The partitioning between liquid and solid hydrometeors is relatively independent of the vertical position within the cloud. However, the mean temperature is related to the liquid water fraction. In the observed clouds, the liquid water fraction is close to 100% at temperatures warmer than −10°C. For synoptic snow clouds, on the other hand, both liquid water drops and ice particles often have grown big enough to fall against updrafts. This vertical "mixing" of particles complicates the partitioning between liquid and ice water. However, within the cloud layer, there still seems to be a tendency for the liquid water fraction to be greater at warmer temperatures (lower altitudes). Due to falling ice particles, the liquid water fraction is only about 50% near 0°C. Based on our study, we conclude that for numerical modeling and/or remote sensing applications it is inappropriate to apply the same liquid–ice partitioning formula uniformly to all clouds, but rather the partitioning should be sorted by cloud type. Of course, more in situ observational data need to be accumulated to solidify the partitioning formula.

5. Conclusions

This work presents a study of various mixed-phase clouds in midlatitudes, particularly the vertical profiles

using in situ aircraft observations that are suited to making direct measurements of cloud properties. The distribution of liquid and ice water with height and temperature is examined for in situ probe measurements during cold seasons from two field campaigns, CLEX-9 and CLEX-10/C3VP. For accurate estimation of the vertical distribution of microphysical quantities within a cloud layer, all flight segments that were obtained by ascending or descending flights through clouds were examined using airborne radar images and the detailed flight tracks. Thirty-four profiles were selected. For three cloud categories (shallow midlevel, deep midlevel, and synoptic snow/convective clouds), LWP and TWP, as well as cloud depth, were obtained and their averaged values are $\sim$39.16–77.71 g m^{-2} for LWP, $\sim$46.81–241.92 g m^{-2} for TWP, and $\sim$0.66–5.26 km for cloud depth. The vertical distributions of LWC and IWC with real altitude and normalized height in each cloud layer with respect to cloud top and base are also shown, as well as with temperature. Of the 34 cloud profiles, 18 were less than 1 km thick. The shallower clouds (shallow midlevel with average depth of 0.66 km) had the highest liquid water fractions ($>$80%), while the deeper cloud profiles contained more ice than liquid. The total liquid water fractions (LWP/TWP) for deep midlevel clouds and synoptic snow clouds were 70% and 35%, respectively. For midlevel cloud profiles, the highest amounts of liquid water exist near cloud top, compared with the synoptic snow cloud profiles where supercooled liquid water increases as height decreases. This is to be expected assuming the clouds are formed in adiabatic ascent. The majority of the midlevel, mixed-phase cloud profiles was quasi-adiabatic, although the composite profiles showed the LWC was typically less than the adiabatic values, likely due to the presence of ice, entrainment, and other environmental factors. The shallow midlevel profiles, which had the highest liquid water fraction, were closest to the adiabatic values.

The use of temperature thresholds and simple relationships between liquid water fraction and temperature is common in the numerical models and remote sensing retrieval algorithms. Previous studies show that the amount of supercooled liquid water in mixed-phase clouds is related to the amount of ice nuclei and/or ice particles, the supply of water vapor, large- (synoptic) and small-scale (turbulent) vertical motions, and radiative heating (Pinto 1998; Rauber and Tokay 1991; Hogan et al. 2002; Korolev and Isaac 2003; Larson et al. 2006; Korolev and Field 2008; Shupe et al. 2008). Unfortunately, these quantities are difficult to observe from remote sensing platforms or simulate numerically on a global scale with sufficient accuracy and resolution. The results of this study show that the liquid–ice water

partitioning depends heavily on cloud type. It is found that the partitioning between liquid and solid hydrometeors for midlevel shallow clouds is relatively independent of the vertical position within the cloud. Instead, it is found that the mean temperature of the cloud layer can be used to infer the liquid water fraction. Also, it is frequently found that liquid water fraction is close to 100% at temperatures warmer than $-10°$C in this cloud category. For synoptic snow clouds, however, both liquid water drops and ice particles often have grown great enough to fall against updrafts. Due to falling ice particles, the liquid water fraction is only about 50% near 0°C. The vertical "mixing" reduces any clear partitioning between predominantly liquid and predominantly ice water regions in the cloud, but a slight tendency is still shown that liquid water fraction is greater at warmer temperatures within the cloud layer. Based on this study, it is recommended that for numerical modeling and/or remote sensing applications the liquid–ice partitioning formula should be classified by cloud type. Also, the results indicate that simple, uniform, linear assumptions often applied in some studies may lead to significant uncertainties in cloud retrievals and modeling.

Since a complete vertical profile from flight ascent or descent through an entire cloud layer did not occur frequently during those field experiments, the number of samples is limited, preventing us from drawing any significant statistical conclusions that can be directly applied to model cloud parameterizations. Also, it should be noted that we used a calibration method from Korolev and Strapp (2002) to take into account the residual effect of ice but the measurement uncertainty issue of the probes regarding ice shattering is still an open area of research that needs further investigation. However, it is suggested that the results in this study may help improve our understanding of various mixed-phase clouds in the real atmosphere and would be useful for observational examples of satellite retrievals or case validation of regional-scale model simulations. More in situ aircraft observations such as those from the present study in addition to the previous observational studies are necessary to further quantify the cloud properties and practically improve the cloud formula in numerical models and satellite retrieval algorithms.

REFERENCES

Ansmann, A., and Coauthors, 2008: Influence of Saharan dust on cloud glaciation in southern Morocco during the Saharan Mineral Dust Experiment. *J. Geophys. Res.,* **113,** D04210, doi:10.1029/2007JD008785.

Barker, H. W., A. V. Korolev, D. R. Hudak, J. W. Strapp, K. B. Strawbridge, and M. Wolde, 2008: A comparison between CloudSat and aircraft data for a multilayer, mixed phase cloud system during the Canadian *CloudSat-CALIPSO* Validation Project. *J. Geophys. Res.,* **113,** D00A16, doi:10.1029/2008JD009971.

Boucher, O., H. Le Treut, and M. B. Baker, 1995: Precipitation and radiation modeling in a general circulation model: Introduction of cloud microphysical processes. *J. Geophys. Res.,* **100,** 16 395–16 414.

Carey, L. D., J. Niu, P. Yang, J. A. Kankiewicz, V. E. Larson, and T. H. Vonder Haar, 2008: The vertical profile of liquid and ice water content in midlatitude mixed-phase altocumulus clouds. *J. Appl. Meteor. Climatol.,* **47,** 2487–2495.

Cober, S. G., G. A. Isaac, A. V. Korolev, and J. W. Strapp, 2001: Assessing cloud-phase condition. *J. Appl. Meteor.,* **40,** 1967–1983.

de Boer, G., G. J. Tripoli, and E. W. Eloranta, 2008: Preliminary comparison of *CloudSat*-derived microphysical quantities with ground-based measurements for mixed-phase cloud research in the Arctic. *J. Geophys. Res.,* **113,** D00A06, doi:10.1029/2008JD010029.

DeMott, P. J., and Coauthors, 2010: Predicting global atmospheric ice nuclei distributions and their impacts on climate. *Proc. Natl. Acad. Sci. USA,* **107,** 11 217–11 222.

Fleishauer, R. P., V. E. Larson, and T. H. Vonder Haar, 2002: Observed microphysical structure of midlevel, mixed-phase clouds. *J. Atmos. Sci.,* **59,** 1779–1804.

Gerber, H., B. G. Arends, and A. S. Ackerman, 1994: New microphysics sensor for aircraft use. *Atmos. Res.,* **31,** 235–252.

Gregory, D., and D. Morris, 1996: The sensitivity of climate simulation to the specification of mixed-phase cloud. *Climate Dyn.,* **12,** 641–651.

Gultepe, I., and G. A. Isaac, 1997: Liquid water content and temperature and temperature relationship from aircraft observations and its applicability to GCMs. *J. Climate,* **10,** 446–452.

——, ——, and S. G. Cober, 2002: Cloud microphysical characteristics versus temperature for three Canadian field projects. *Ann. Geophys.,* **20,** 1891–1898.

Heymsfield, A. J., and L. M. Miloshevich, 1993: Homogeneous ice nucleation and supercooled liquid water in orographic wave clouds. *J. Atmos. Sci.,* **50,** 2335–2353.

——, ——, C. Schmitt, A. Bansemer, C. Twohy, M. R. Poellot, A. Fridland, and H. Gerber, 2005: Homogeneous ice nucleation in subtropical convection and its influence on cirrus anvil microphysics. *J. Atmos. Sci.,* **62,** 41–64.

Hogan, R. J., P. R. Field, A. J. Illingworth, R. J. Cotton, and T. W. Choularton, 2002: Properties of embedded convection in warm-frontal mixed-phase cloud from aircraft and polarimetric radar. *Quart. J. Roy. Meteor. Soc.,* **128,** 451–476.

——, A. J. Illingworth, E. J. O'Connor, and J. P. V. Poiares Baptista, 2003: Characteristics of mixed-phase clouds. II: A climatology from ground-based lidar. *Quart. J. Roy. Meteor. Soc.,* **129,** 2117–2134.

Houghton, R. A., K. T. Lawrence, J. L. Hackler, and S. Brown, 2001: The spatial distribution of forest biomass in the Brazilian Amazon: A comparison of estimates. *Global Change Biol.,* **7,** 731–746.

Houze, R. A., Jr., 1993: *Cloud Dynamics.* Academic Press, 573 pp.

Hu, Y., S. Rodier, K. Xu, W. Sun, J. Huang, B. Lin, P. Zhai, and D. Josset, 2010: Occurrence, liquid water content, and fraction of supercooled water clouds from combined CALIOP/IIR/MODIS measurements. *J. Geophys. Res.,* **115,** D00H34, doi:10.1029/2009JD012384.

King, W. D., D. A. Parkin, and R. J. Handsworth, 1978: A hot-wire water device having fully calculable response characteristics. *J. Appl. Meteor.,* **17,** 1809–1813.

Knollenberg, R. G., 1981: Techniques for probing cloud microstructure. *Clouds: Their Formation, Optical Properties, and Effects,* P. V. Hobbs and A. Deepak, Eds., Academic Press, 15–89.

Korolev, A. V., and J. W. Strapp, 2002: Accuracy of measurements of cloud ice water content by the Nevzorov probe. Preprints, *40th Aerospace Sciences Meeting and Exhibit,* Reno, NV, AIAA 2002-0679.

——, and G. Isaac, 2003: Phase transformation of mixed-phase clouds. *Quart. J. Roy. Meteor. Soc.,* **129,** 19–38.

——, and P. R. Field, 2008: The effect of dynamics on mixed-phase clouds: Theoretical considerations. *J. Atmos. Sci.,* **65,** 66–86.

——, J. W. Strapp, G. A. Isaac, and A. N. Nevzorov, 1998: The Nevzorov airborne hot-wire LWC-TWC probe: Principle of operation and performance characteristics. *J. Atmos. Oceanic Technol.,* **15,** 1495–1510.

——, G. A. Isaac, S. G. Cober, J. W. Strapp, and J. Hallett, 2003: Microphysical characterization of mixed-phase clouds. *Quart. J. Roy. Meteor. Soc.,* **129,** 39–65.

——, ——, J. W. Strapp, S. G. Cober, and H. Barker, 2007: In-situ measurements of liquid water content profiles in mid-latitude stratiform clouds. *Quart. J. Roy. Meteor. Soc.,* **133,** 1693–1699.

——, J. W. Strapp, G. A. Isaac, and E. Emery, 2008: Improved airborne hot-wire measurements of ice water content in clouds. *Proc. 15th Int. Conf. on Clouds and Precipitation,* Cancun, Mexico, Int. Assoc. of Meteorology and Atmospheric Science, 9 pp. [Available online at http://cabernet.atmosfcu.unam.mx/ICCP-2008/abstracts/Program_on_line/Poster_13/Korolev_extended_4.pdf.]

Larson, V. E., A. J. Smith, M. J. Faulk, K. E. Kotenberg, and J.-C. Golaz, 2006: What determines altocumulus dissipation time? *J. Geophys. Res.,* **111,** D19207, doi:10.1029/2005JD007002.

Mazin, I. P., 2006: Cloud phase structure: Experimental data analysis and parameterization. *J. Atmos. Sci.,* **63,** 667–681.

Mitchell, D. L., R. Zhang, and R. Pitter, 1990: Mass-dimensional relationships for ice particles and the influence of riming on snowfall rate. *J. Appl. Meteor.,* **29,** 153–163.

Niu, J., L. D. Carey, P. Yang, and T. H. Vonder Haar, 2008: Optical properties of a vertically inhomogeneous mid-latitude mid-level mixed-phase altocumulus in the infrared region. *Atmos. Res.,* **88,** 234–242.

Noh, Y. J., C. J. Seaman, T. H. Vonder Haar, D. R. Hudak, and P. Rodriguez, 2011: Comparisons and analyses of wintertime mixed-phase clouds using satellite and aircraft observations. *J. Geophys. Res.,* **116,** D18207, doi:10.1029/2010JD015420.

Pinto, J. O., 1998: Autumnal mixed-phase cloudy boundary layers in the Arctic. *J. Atmos. Sci.,* **55,** 2016–2037.

Platt, C. M. R., 1977: Lidar observation of a mixed-phase altostratus cloud. *J. Appl. Meteor.,* **16,** 339–345.

Randall, D. A., and Coauthors, 2007: Climate models and their evaluation. *Climate Change 2007: The Physical Science Basis,* S. Solomon et al., Eds., Cambridge University Press, 589–662.

Rauber, R. M., and A. Tokay, 1991: An explanation for the existence of supercooled water at the tops of cold clouds. *J. Atmos. Sci.,* **48,** 1005–1023.

Rogers, R. R., and M. K. Yau, 1989: *A Short Course in Cloud Physics.* 3rd ed. Butterworth-Heinemann, 290 pp.

Shupe, M. D., 2007: A ground-based multiple remote-sensor cloud phase classifier. *Geophys. Res. Lett.,* **34,** L22809, doi:10.1029/2007GL031008.

——, S. Y. Matrosov, and T. Uttal, 2006: Arctic mixed-phase cloud properties derived from surface-based sensors at SHEBA. *J. Atmos. Sci.,* **63,** 697–711.

——, P. Kollias, P. Ola, G. Persson, and G. M. McFarquhar, 2008: Vertical motions in Arctic mixed-phase stratiform clouds. *J. Atmos. Sci.,* **65,** 1304–1322.

Smith, R. N. B., 1990: A scheme for predicting layer clouds and their water content in a general circulation model. *Quart. J. Roy. Meteor. Soc.,* **116,** 435–460.

Sun, Z., and K. P. Shine, 1994: Studies of radiative properties of ice and mixed phase clouds. *Quart. J. Roy. Meteor. Soc.,* **120,** 111–137.

——, and ——, 1995: Parameterization of ice cloud radiative properties and its application to the potential climatic importance of mixed-phase clouds. *J. Climate,* **8,** 1874–1888.

Swanson, B. D., 2009: How well does water activity determine homogeneous ice nucleation temperature in aqueous sulfuric acid and ammonium sulfate droplets? *J. Atmos. Sci.,* **66,** 741–754.

Tiedtke, M., 1993: Representation of clouds in large-scale models. *Mon. Wea. Rev.,* **121,** 3040–3061.

Wang, Z., K. Sassen, D. N. Whiteman, and B. B. Demoz, 2004: Studying altocumulus with ice virga using ground-based active and passive remote sensors. *J. Appl. Meteor.,* **43,** 449–460.

Zhang, D., Z. Wang, and D. Liu, 2010: A global view of mid-level liquid-layer topped stratiform cloud distribution and phase partition from *CALIPSO* and *CloudSat* measurements. *J. Geophys. Res.,* **115,** D00H13, doi:10.1029/2009JD012143.

Zuidema, P., and Coauthors, 2005: An Arctic springtime mixed-phase cloudy boundary layer observed during SHEBA. *J. Atmos. Sci.,* **62,** 160–176.